

JET-P(93)66

M. Ottaviani, F. Porcelli

Nonlinear Collisionless Magnetic Reconnection

“This document contains JET information in a form not yet suitable for publication. The report has been prepared primarily for discussion and information within the JET Project and the Associations. It must not be quoted in publications or in Abstract Journals. External distribution requires approval from the Publications Officer, JET Joint Undertaking, Abingdon, Oxon, OX14 3EA, UK”.

“Enquiries about Copyright and reproduction should be addressed to the Publications Officer, EFDA, Culham Science Centre, Abingdon, Oxon, OX14 3DB, UK.”

The contents of this preprint and all other JET EFDA Preprints and Conference Papers are available to view online free at www.iop.org/Jet. This site has full search facilities and e-mail alert options. The diagrams contained within the PDFs on this site are hyperlinked from the year 1996 onwards.

Nonlinear Collisionless Magnetic Reconnection

M. Ottaviani, F. Porcelli

JET-Joint Undertaking, Culham Science Centre, OX14 3DB, Abingdon, UK

Preprint of a paper to be submitted for publication in
Physical Review Letters
September 1993

ABSTRACT

Collisionless magnetic reconnection in regimes where the mode structure is characterised by global convection cells is found to exhibit a quasi-explosive time behaviour in the early nonlinear stage where the fluid displacement is smaller than the equilibrium scale length. This process is accompanied by the formation of a current density sub-layer narrower than the skin depth. This sublayer keeps shrinking with time.

Magnetic reconnection in collisionless regimes, where electron inertia is responsible for the decoupling of the plasma motion from that of the magnetic field, is a well known process in Astrophysics¹. It is quite exciting that this process can now be observed in laboratory plasmas produced by Tokamaks such as the Joint European Torus (JET). Indeed, at the high plasma temperatures of these experiments, internal plasma relaxation oscillations (the so-called² *sawteeth*) can occur on a time scale shorter than the electron-ion collision time. Motivated by these observations, the linear theory of $m=1$ kink-tearing modes, which trigger the sawtooth relaxations, has recently been extended to experimentally relevant regimes³⁻⁶, leading to the conclusion that these modes can remain virulent at low collisionality with an initial growth rate which compares favourably with that observed in the experiments. However, the nonlinear evolution has remained unclear. While Wesson's⁷ modification of the Sweet-Parker-Kadomtsev⁸⁻¹⁰ scaling has given an estimate of the collisionless reconnection time in good agreement with that observed experimentally, Drake & Kleva's numerical simulation¹¹ of the merging of two isolated flux bundles has led to the suggestion that the collisionless reconnection rate is greatly reduced as the nonlinear phase is entered, i.e. for magnetic island widths comparable with the plasma skin depth.

With the aim of clarifying these issues, we present the numerical and analytic solution of a collisionless, incompressible, 2-D slab model where Larmor radius effects are neglected. The equations we solve are

$$\partial_t U + [\varphi, U] = [J, \psi], \quad (1)$$

$$\partial_t F + [\varphi, F] = 0, \quad (2)$$

where we use the notation $\partial_t \equiv \partial/\partial t$ and $[A, B] \equiv \mathbf{e}_z \cdot \nabla A \times \nabla B$, with \mathbf{e}_z the unit vector along the z direction. $U = \nabla^2 \varphi$ is the fluid vorticity, φ is the stream function, $\mathbf{v} = \mathbf{e}_z \times \nabla \varphi$ is the fluid velocity, $J = -\nabla^2 \psi$ is the current density along z , ψ is the magnetic flux function and $F \equiv \psi + d^2 J$, with d the skin depth. Thus, $[\varphi, F] = \mathbf{v} \cdot \nabla F$ and the collisionless Ohm law (2) can be written as $dF/dt = 0$, i.e. F is conserved on a moving fluid element. The co-ordinate z is ignorable, $\partial_z = 0$. The co-ordinates x and y vary in the intervals $x \in [-L_x, L_x]$ and $y \in [-L_y, L_y]$, with the slab aspect ratio $\varepsilon \equiv L_x/L_y < 1$. Periodic boundary conditions are imposed at the edge of these intervals. The magnetic field is $\mathbf{B} = B_0 \mathbf{e}_z + \nabla \psi \times \mathbf{e}_z$, with B_0 a constant value which we take to scale as $B_0 \sim \varepsilon^{-1} |\nabla \psi|$ in order to mimic the magnetic field of a Tokamak. All quantities in Eqs. (1,2) are dimensionless, with L_x and $\tau_A = (4\pi\rho_m)^{1/2} L_x / B_0$ determining the length and time scale normalisation.

We consider an equilibrium specified by $L_x = \pi$, $\varphi_0 = U_0 = 0$, $J_0 = \psi_0 = \cos x$, and $F_0 = (1 + d^2) \psi_0$. This equilibrium is tearing-unstable to linear perturbations of the type $(\varphi, \delta\psi) = \text{Real}\{[\varphi_L(x), \delta\psi_L(x)]e^{\gamma t + iky}\}$, with $k = m\varepsilon$ and m an integer number, and with $\varphi_L(x)$ and $\delta\psi_L(x)$ respectively odd and even functions around the two equivalent reconnecting surfaces at $x = 0$ and at $x = \pm L_x$. In the limit $d \ll L_x$, the solution of the linearized system can be obtained analytically using asymptotic matching techniques. For $0 < k^2 \leq 1$, the linearized mode structure in the *outer* region is $\delta\psi_L = \psi_\infty \cos[\kappa(|x| - \pi/2)]$ and $\varphi_L = (i\gamma/k \sin x) \delta\psi_L$, with ψ_∞ a constant and $\kappa \equiv (1 - k^2)^{1/2}$. The logarithmic jump of $\delta\psi_L$ across the reconnecting layers is $\Delta' = 2\kappa \tan(\kappa\pi/2)$. We consider the *large- Δ'* regime, defined by

$$\Delta' d \geq 1, \quad (3)$$

which can be satisfied for low values of m and $\varepsilon^2 \ll 1$ such that $\Delta' \sim (8/\pi k^2)$. In this regime, the structure of the stream function is macroscopic, with $\varphi_L \approx \varphi_\infty \text{sign} x$, $\varphi_\infty \equiv (i\gamma/k) \psi_\infty$, everywhere except in narrow layers near the reconnecting surfaces. For $\Delta' d \gg 1$, the eigenfunctions in the vicinity of the layer at $x=0$ take the form $\delta J_L \approx -\psi_\infty (2/\pi d^2)^{1/2} \exp(-x^2/2d^2)$ and $\varphi_L \approx \varphi_\infty \text{erf}(x/2^{1/2}d)$, which match onto the outer solution for $|x| > d$. Thus, the current channel in the linear stage has a width $\delta_L \sim d$. The linear growth rate is $\gamma_L \approx kd$.

The system of Eqs. (1,2) is solved numerically with a pseudospectral code¹² which advances in time the Fourier representation of the field variables, truncated to 1024×64 (x, y) components. We are interested in the early nonlinear phase, defined by the condition $d < w < 2L_x$, where w is the magnetic island width. The initial conditions are chosen to approximate closely the linear eigenfunctions, and in particular to reproduce the spatial symmetries of the linear solution around the X- and O-points and the reflection symmetry with respect to the four points $x = \pm L_x / 2$, $y = \pm L_y / 2$. It can be easily verified by inspection of (1,2) that these symmetries are preserved during the nonlinear evolution. An important consequence is that the value of F at $x = 0$ is frozen to its initial value, i.e. $F(x = 0, y, t) = F_0(x = 0) = 1 + d^2$.

For $\varepsilon \ll 1$, the adopted equilibrium is linearly unstable to several mode-numbers, m . On the other hand, in the numerical analysis of the full non-linear system (1,2), it is convenient to follow the evolution of a single linearly unstable mode. This requirement is dictated both by reasons of simplicity and by analogy with the kink-tearing instability in a toroidal plasma. Therefore, we present numerical runs with $\varepsilon = 0.5$ and $d / (2L_x) = 0.04$, which give $d\Delta' \approx 2.03$ for $m = 1$, thus satisfying the large- Δ' condition (3), while the other m -values are stable ($\Delta' \leq 0$ for $m \geq 2$). Figure 1 shows sections of $\delta\psi \equiv \psi - \psi_0$, $v_x = -\partial\phi / \partial y$, J and F across the X-point ($y = 0$) at various times. The linear phase conventionally lasts until $t \sim 80$, when the magnetic island reaches a width of order d . The linear layer width $\sim d$ is visible from these graphs. For $t > 80$, the width of the profile of v_x , $\delta\phi \equiv (v_x)_{x=L_x/2} / (\partial_x v_x)_{x=0}$, as well as that of $\delta\psi$, remain of the order of the skin depth (Figs. 1a,b). By contrast, the current density profile (Fig. 1c) develops a sub-layer whose width around the X-point, $\delta_J \equiv (\partial_x^2 \delta J / \delta J)^{-1/2} < d$, keeps shrinking with time (see also Fig. 2d). Here, $\delta J \equiv J - J_0$. This sub-layer is also visible in the profile of F across the X-point (Fig. 1d). The contraction of this sub-layer is extremely rapid in time, as shown by the graph of $\partial^2 F / \partial x^2$ versus y for $x = 0$ and several times in Fig. 2b. At $t \approx 125$, it has become so narrow that it can no longer be resolved by our truncated Fourier expansion, and so the simulation is stopped. Also shown in Fig. 2a and 2c are the profiles of $\delta\psi$ and of $v_y = \partial\phi / \partial x$ along the reconnection line ($x = 0$) at various times, from which it is clear that only a limited number of Fourier harmonics along y are involved in the early non-linear evolution. Contour plots of ϕ , ψ , J and F are shown in Fig. 3. Note that the convection cells retain approximately their linear shape well into the nonlinear phase (Fig. 3a). Also note the development of a current sheet around

the reconnection line (Fig. 3c) and the preservation of the topology of the isolines of F (Fig. 3d). Finally, Fig. 4 summarizes the time behaviour. It is remarkable that the mode growth remains very rapid throughout the simulation. Indeed, the growth of φ , as well as that of $\delta\psi$ and δI at the X-points, accelerate in the early nonlinear phase, which is symptomatic of an explosive behaviour. However, the mode growth slows down when w approaches L_x , as we have observed in a simulation with $d/(2L_x) = 0.08$ (not shown here).

According to these numerical results, the spatial structure of the stream function does not vary significantly with time throughout the linear and early nonlinear phases. This suggests that we can write

$$\varphi(x, y, t) = v_o(t)g(x)h(y) + u(x, y, t) \quad (4)$$

where $h(y) \sim k^{-1} \sin(ky)$, $g(x) \sim \varphi_L(x)/\varphi_\infty$ contains the linear scale length d and $u(x, y, t)$ develops the rapid scale length $\delta(t) \sim \delta_I$ observed in the numerical simulation. We assume $u \ll v_o$ and $\partial_x u \sim v_o \partial_x g$, which is consistent with the near constancy in time of the width of v_x across the reconnecting layer (Fig. 2d), as well as that of the ratio $v_y(0, L_y/2, t)/v_x(-L_x/2, 0, t)$ (Fig. 4). These assumptions allow an analytic treatment of the system of Eqs. (1,2).

The collisionless Ohm's law (2) can be integrated exactly to yield $F = F_o(x_o)$, where $x_o(x, y, t) = x - \xi(x, y, t)$ is the initial position of a fluid element situated at (x, y) at time t and ξ is the displacement along the x direction defined by the equation $d\xi/dt = v_x$, $\xi(t = -\infty) = 0$. The latter equation can be integrated using the methods of the characteristics. At $y = 0$, where v_y vanishes, using the ansatz (4) where $u(x, y, t)$ can be neglected, we find

$$-\int_{x_o}^x dx'/g(x') = \int_{-\infty}^t v_o(t') dt' \equiv \lambda(t). \quad (5)$$

The function $\lambda(t) > 0$ represents the amplitude of ξ outside the reconnection layer, where $g(x) \approx 1$. In the linear phase, $-\psi_\infty \approx \lambda < d$. When $\lambda > d$, the magnetic island width $w \sim 2\lambda$, so that the early nonlinear phase can also be characterised by the inequality $d < \lambda < L_x$, or alternatively $t_0 < t < t_D$, with $\lambda(t_0) \sim d$ and t_D the characteristic turnover time of the macroscopic eddies in Fig. 3a.

Equation (5) can be inverted to obtain $x_o = x_o(x, t)$. In the limit $d < \lambda < L_x$, the time-dependent scale length is found,

$$\delta(t) \equiv d \exp[-\lambda(t)/d], \quad (6)$$

such that x_o has the following behaviour around $y=0$: $x_o \sim (x/\delta)\hat{d}$ for $|x| < \delta$; $x_o \sim [\lambda + \hat{d} \ln(|x|/\hat{d})] \text{sign}(x)$ for $d > |x| > \delta$; and $x_o \sim \lambda \text{sign}(x) + x$ for $|x| > d$, where $\hat{d} \equiv (dg/dx)_{x=0}^{-1} \sim d$. Thus we see that near the X-point along the x direction, $F(x_o)$ (and hence J) varies over a distance $\delta(t)$ which becomes exponentially small in the ratio λ/d . Conversely, around $y = \pm L_y$, $\lambda \rightarrow -\lambda$ in Eq. (5). Then, $x_o < d$ for $|x| < \lambda$ and F flattens over a distance $|x| \sim \lambda$ from the O-point. We stress that the formation of a sub-layer is the combined result of the conservation of F on each fluid element and the flow pattern around the X-point, which acts to increase the local curvature of the F profile (Fig. 1d).

Next, we obtain an expression for ψ by integrating the equation $\psi + d^2 J = F$, where we can approximate $J \approx -\partial_x^2 \psi$. Using as asymptotic boundary condition the matching of $\delta\psi$ to the linear solution for $\lambda < |x| < L_x$, we obtain $\psi(x, y, t) \approx \frac{1}{2} \int_{-\infty}^{\infty} e^{-|\hat{x}-\hat{x}'|} F(\hat{x}', y, t) d\hat{x}'$, where $\hat{x} \equiv x/d$, which shows that ψ has an integral structure such that any fine scale variation of F is smoothed out over a distance $\sim d$. Asymptotic evaluation of ψ at the X- and O-points in the early nonlinear phase gives

$$\psi_X \equiv \psi(0, 0, t) \sim 1 - \frac{1}{2} \lambda^2(t), \quad \psi_O \equiv \psi(0, \pm L_y, t) \sim 1 + O(d^2). \quad (7)$$

Let us set $F = F_o(x) + \delta F$. Then, $\delta\psi + d^2 \delta J = \delta F$, and at $x=0$, where $\delta F = 0$, we find $\delta J = -\delta\psi/d^2$. Thus we have demonstrated that an asymmetry develops in the values of $\delta\psi$ and of J between the X- and O-points. The spike of the current density at the X-point has an amplitude $\delta J_X \sim 0.5(\lambda/d)^2$.

Let us now integrate the vorticity equation (1) over the quadrant $S: [0 \leq x \leq L_x, 0 \leq y \leq L_y]$, such that $\int_S [\phi, U] dx dy = 0$. Using Stokes theorem, we obtain

$$\partial_t \int_S U dx dy = \oint_C J d\psi. \quad (8)$$

where C is the boundary of S . With the ansatz (4), and neglecting corrections $\mathcal{O}(k^2 d^2)$ contributed by $\partial_y^2 \phi$, we find

$$\partial_t \int_S (\partial_x^2 \phi) dx dy \approx - (4c_0 c_1 / k^2 d) d^2 \lambda / dt^2, \quad (9)$$

where $c_0 = d / \hat{d} = \mathcal{O}(1)$ and $c_1(t) = 1 + (d / c_0 v_o) (\partial_x u)_X$ is a factor of order unity, which depends weakly on time (e.g. $1 \leq c_1 \leq 1.4$ in Fig. 2d). Exploiting the reflection symmetry with respect to $x = L_x / 2$, $y = L_y / 2$, the second integral in Eq. (8) can be written as

$$\oint_C J d\psi = -2 \int_0^{L_y} dy (J \partial_y \psi)_{x=0} - 2 \int_0^{L_x} dx \left[(\partial_y^2 \psi) (\partial_x \psi) \right]_{y=0}$$

The first integral at the right hand side can be evaluated exactly:

$$-\int_0^{L_y} dy (J \partial_y \psi)_{x=0} = \delta\psi_X - \delta\psi_O - (\delta\psi_X^2 - \delta\psi_O^2) / 2d^2. \quad (10)$$

The second integral gives a contribution of order $k^2 \lambda$, which is negligible when $\Delta' d \sim 8d / \pi k^2 > 1$, and which is significant only in the linear phase when $\Delta' d \sim 1$.

Using an interpolation formula between the linear and early nonlinear limits of the r.h.s. of (10), and inserting this and (9) into (8), we obtain an equation for the evolution of $\hat{\lambda}(t) \equiv \lambda(t) / d$:

$$d^2 \hat{\lambda} / dt^2 \approx \hat{\lambda} + c_2 \hat{\lambda}^4 \quad (11)$$

where $\hat{t} \equiv \gamma_L t$ and $c_2 \approx 1 / 16 c_0 c_1$ can be taken constant. The solution is $\hat{\lambda}(\hat{t}) = \left[(1 - \alpha) / (1 - \alpha e^{3\hat{t}}) \right]^{2/3} e^{\hat{t}}$, where $\alpha = \beta - (\beta^2 - 1)^{1/2}$, $\beta = 1 + 5 / c_2$, and we have chosen the time origin so that $\hat{\lambda}(0) \equiv 1$. Thus, once the early nonlinear regime is entered, $\lambda(t)$ accelerates and reaches a macroscopic size over a fraction $\sim \ln(\alpha^{-1/3})$ of the linear growth time. As we remarked earlier, we can expect this quasi-explosive growth to cease as λ approaches L_x .

In conclusion, collisionless reconnection in regimes where the instability parameter Δ' is large and global convection cells develop does not follow the

standard Sweet-Parker scenario^{8,9}. In these regimes, the reconnection rate accelerates nonlinearly. Physically, the flow rotation accelerates following the intensification of the electromagnetic torque $\oint_C \mathbf{J} \times \mathbf{B} \cdot d\mathbf{l} = \oint_C J d\psi$ in the early nonlinear regime. This torque is mainly contributed by the average $J_x B_x$ force between the X- and O-points within a magnetic island, corresponding to the integral of Eq. (10). The current density profile develops a sub-layer narrower than the skin depth. The formation of a narrow scale length less than the skin depth was also noted by Wesson⁷ and by Drake & Kleva¹¹. However, these authors' analyses do not take properly into account the multiple scale structure of the current density and flow profiles. In particular, we find that the conclusion in Ref. 11 that the reconnection rate slows down nonlinearly is not justified when the magnetic island has a width larger than the skin depth but smaller than the size of the convection cells.

As an extremely narrow current spike develops during the reconnection process, the electron distribution function tends to become highly distorted and one can think of instabilities which would limit this tendency, introducing an effective ("anomalous") current diffusion. Clearly, a refined model is needed to describe this for realistic experimental parameters, with effects such as the finite ion Larmor radius, density and pressure gradients, 3-D, etc. likely to play an important role. Nevertheless, we believe that the present analysis opens the possibility to understand the rapidity of relaxation processes observed in low collisionality plasmas.

The authors would like to thank John Wesson for stimulating discussions.

REFERENCES

- [1] V.M.Vasyliunas, *Rev. Geophys. Space Phys.* **13**, 303 (1975).
- [2] A.W.Edwards et al, *Phys. Rev. Lett.* **57**, 210 (1986).
- [3] F.Porcelli, *Phys. Rev. Lett.* **66**, 425 (1991).
- [4] H.L.Berk, S.M.Mahajan and Y.Z.Zhang, *Phys.Fluids* **B3**, 351 (1991).
- [5] B.Coppi and P.Detragiache, *Phys. Lett.* **A168**, 59 (1992).
- [6] L.E.Zakharov and B.Rogers, *Phys. Fluids* **B4**, 3285 (1992).
- [7] J.Wesson, *Nuclear Fusion* **30**, 2545 (1990).
- [8] P.A.Sweet, in *Electromagnetic Phenomena in Cosmic Physics*, ed. by B.Lehnert (Cambridge University Press, 1958), p. 123.
- [9] E.N.Parker, *J. Geophys. Research* **62**, 509 (1957).
- [10] B.B.Kadomtsev, *Fiz. Plasmy* **1**, 710 (1975) [*Sov. J. Plasma Phys.* **1**, 389 (1975)]
- [11] J.F.Drake and R.G.Kleva, *Phys. Rev. Lett.* **66**, 1458 (1991).
- [12] S.A.Orszag and G.S.Patterson, *Phys. Rev. Lett.* **28**, 76 (1972).

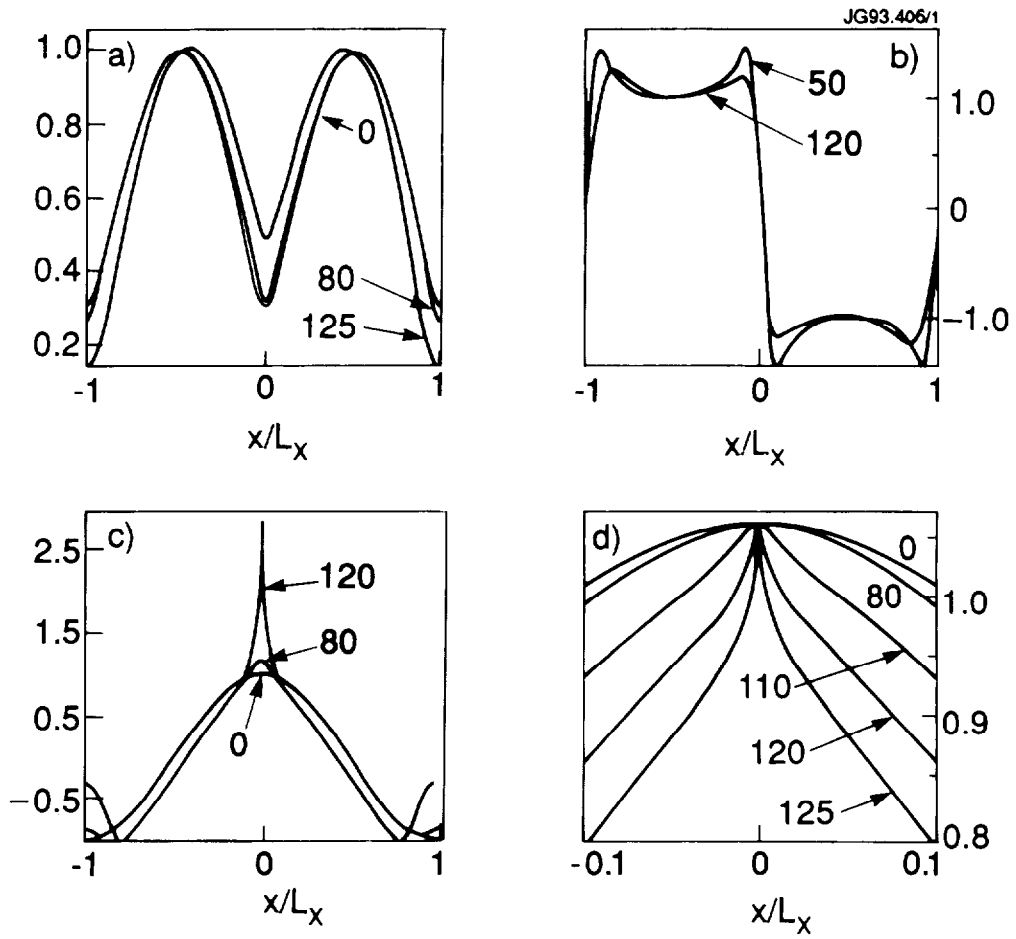


Fig. 1. Cross sections of a) $\delta\psi / (\delta\psi)_{x=L_x/2}$; b) $v_x / (v_x)_{x=-L_x/2}$; c) J ; d) F versus x at $y=0$. The X-point is at $x=0$; the O-point of the second island chain is at $x=\pm L_x$. Times are indicated by the arrows.

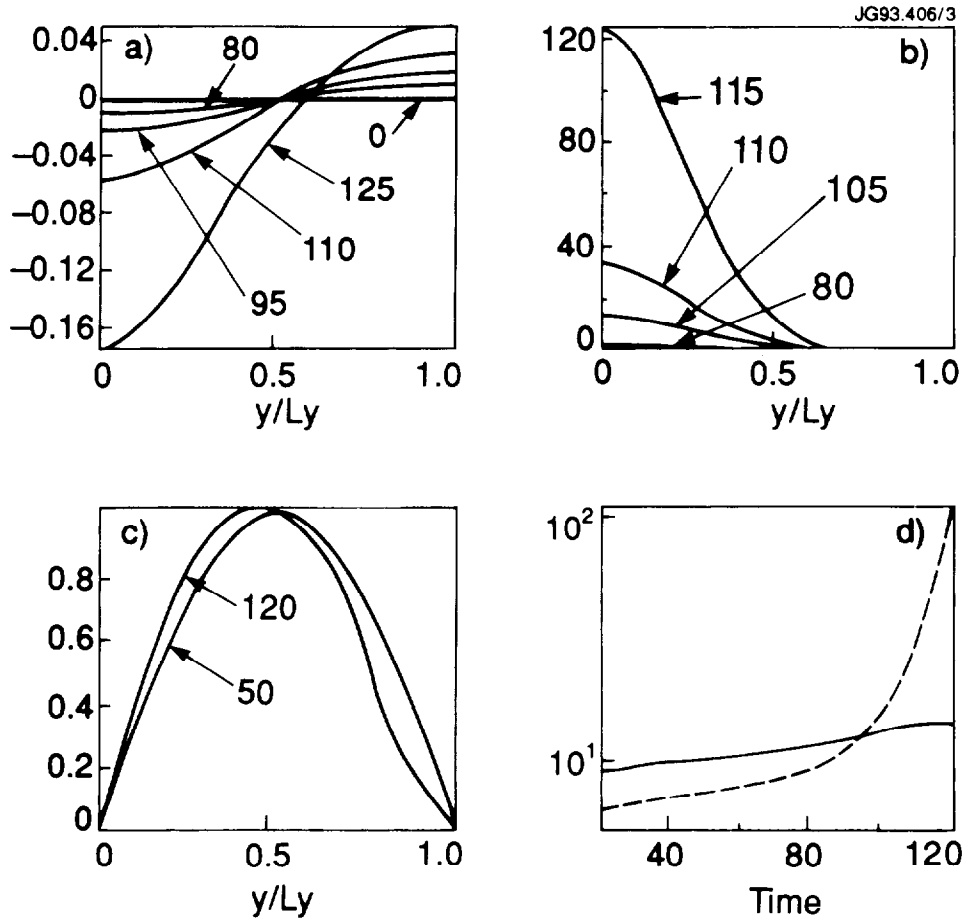


Fig. 2. Cross sections of a) $\delta\psi$; b) $\partial^2 F / \partial x^2$; c) $v_y / (v_y)_{y=L_y/2}$ versus y at $x=0$. The island's X- and O-points are at $y=0$ and $y=L_y$, respectively. Also, d) time dependence of the logarithm of the inverse scale lengths δ_ϕ^{-1} (solid line) and δ_j^{-1} (broken line).

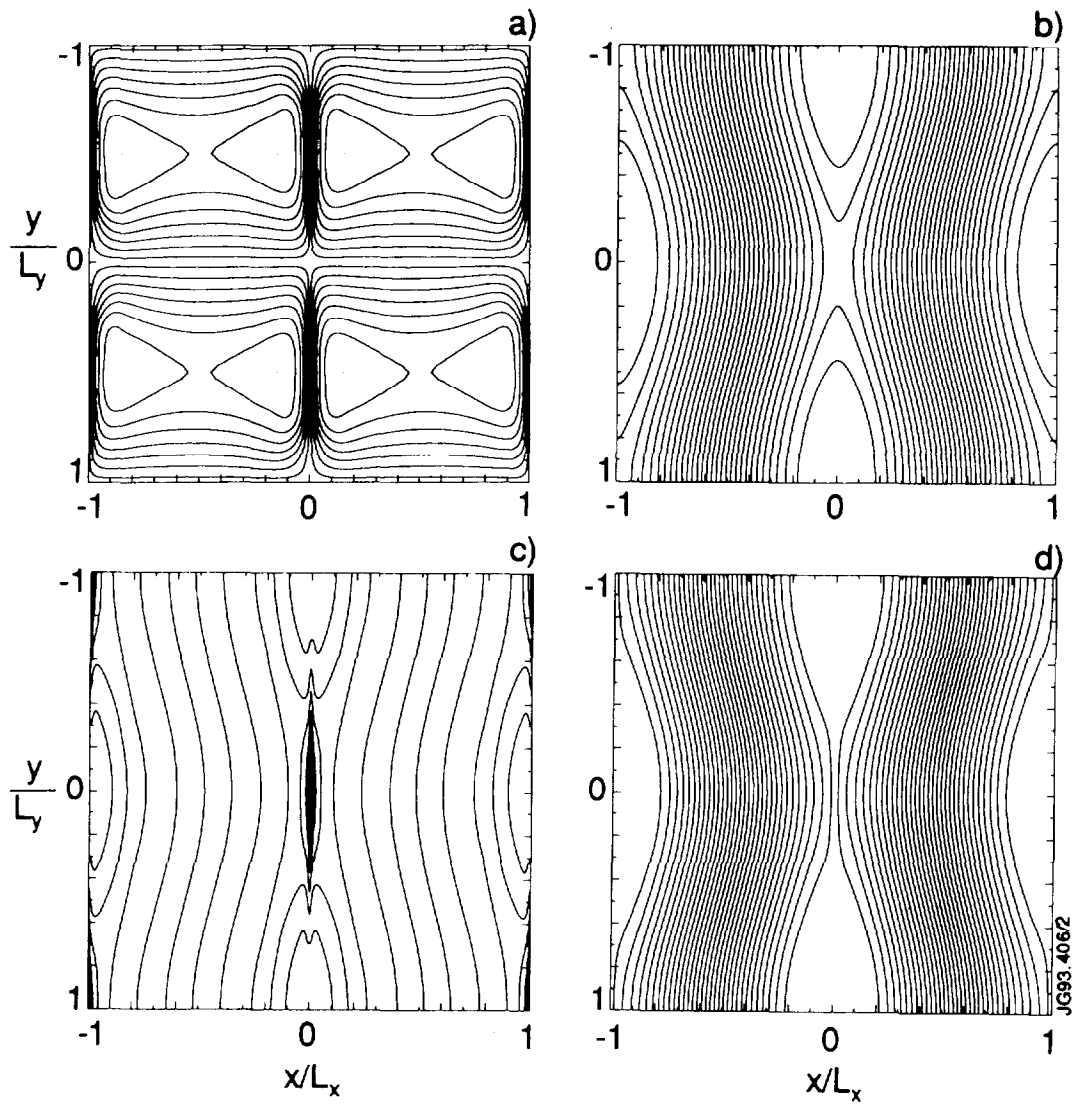


Fig. 3. Contour plots at $t=120$: a) φ ; b) ψ ; c) J ; d) F .

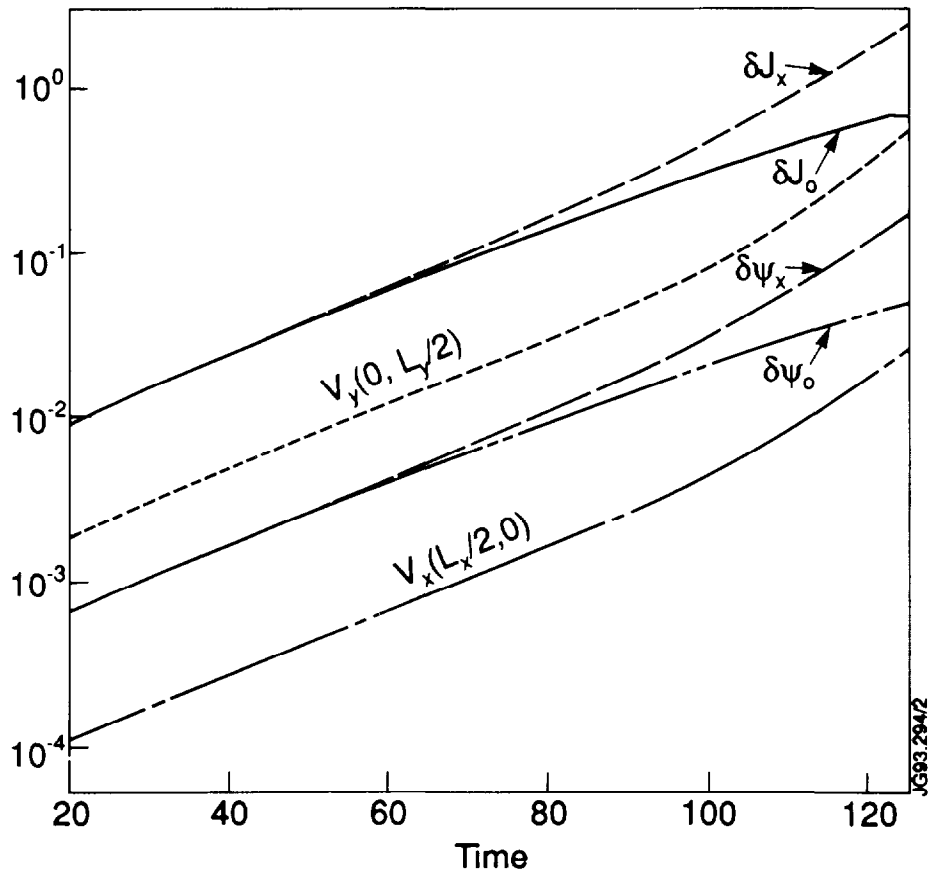


Fig. 4. Time dependence of $\delta\psi$ and δI at the X- and O-points, of $v_x(-L_x/2, 0)$ and of $v_y(0, L_y/2)$.